

Self-similar cosmological expansion of collisional gas

Leonid Chuzhoy and Adi Nusser

Physics Department, Technion, Haifa 32000, Israel

E-mail: cleonid@tx.technion.ac.il, adi@physics.technion.ac.il

26 October 2018

ABSTRACT

We derive similarity solutions for the expansion of negative initial density perturbations $\delta M/M \propto r^{-s}$ ($s > 0$) in an Einstein-de Sitter universe filled with collisional baryonic gas and collisionless matter. The solutions are obtained for planar, cylindrical, and spherical perturbations. For steep perturbations, central cavities surrounded by over-dense shells expanding as $t^{2(s+1)/(3s)}$ develop in both matter components. We also consider the case when baryonic shells are driven by internal pressure. Before redshift $\sim 8 - 10$ baryonic shells cool by inverse Compton scattering with the cosmic background radiation and can form bound objects of mass $\sim 10^{11} \Omega_b^{-1/2} M_\odot (1+z)^{-3/2}$. Hot shocks of radius R cause a Compton y -distortion of order $y = 10^{-5} \Omega_b (R/10\text{Mpc})^2 f_F$, where f_F is the volume filling factor of these shells.

Key words: cosmology: theory – gravitation – dark matter – baryons – intergalactic medium

1 INTRODUCTION

Gravitational collapse of matter in initially over-dense regions leads to the formation of dense bound objects in the universe. Star formation is efficient in these objects and so we expect them to harbor most of the luminous matter in the universe. In the linear regime, gravitational instability simply amplifies the density fluctuations by a universal time dependent factor. Thus, an initially under-dense region remains under-dense and cannot lead to the formation of dense structures. In the nonlinear regime, however, the evolution of under-dense regions depends strongly on the profile of its density perturbation. In an isolated under-dense region, the density remains below the background if the profile is shallow. If the profile is steep then expanding inner shells can catch up with shells farther out causing the appearance of caustics in the collisionless matter component and shocks in the baryonic gas (e.g., Fillmore & Goldreich 1984, Bertschinger 1985). Caustics and shocks are very dense and can fragment under their self-gravity to form bound structures.

In a generic density field, a large scale under- or over-dense region contains small scale substructure of density fluctuations. In a large scale over-density, substructures merge under the large scale gravitational field and become part of a large object typically of the mass of the large scale region. Dynamics of under-dense regions can be more complex, depending on the details of the large scale density profile. Over-densities develop into virialized bound objects which are easily identified in observations and N-body

simulations, by means of the friends-of-friends algorithm for example. The fate of under-dense regions however is less certain and strongly depends on the initial conditions. Because of the complexity in studying the dynamics of matter in under-dense regions, analytic solutions for special symmetric negative perturbations are particularly important. Most authors focused on symmetric initial perturbation of the form $\delta M/M \propto r^{-s}$. In a matter dominated flat universe the gravitational evolution of this profile leads to self-similarity, which considerably simplifies the problem. Another simplifying assumption, that is often made for evolution of under-dense system, is that of spherical symmetry. To see the physical motivation for this assumption consider an ellipsoidal top-hat perturbation. Since the perturbing force (acceleration for negative and deceleration for positive perturbation) is stronger along the minor axis, the asymmetry of a void will decrease. Ryden (1994) has investigated the evolution of under-dense collisionless axisymmetric systems with the initial perturbation of the form $\delta M/M \propto r^{-s} f(\Theta)$, where Θ is an angle with the symmetry axis, and found that the emerging void is nearly spherical. Fillmore & Goldreich (1984) have found similarity solutions for spherical perturbations in collisionless matter with $s < 3$, while Bertschinger (1985) obtained solutions for $s = 3$ (uncompensated hole) for both gas and the collisionless matter. However, under certain conditions, the system becomes unstable and spherical symmetry might be destroyed. Several authors have developed different approximations to determine the conditions for instability and to evaluate the sizes of the formed objects (Bertschinger 1983; Vishniac 1983; Hwang, Vishniac and Shapiro 1989; White and Ostriker 1990). In the special case of a compen-

arXiv:astro-ph/0201046v2 24 Dec 2002

sated void (i.e. void surrounded by an over-dense shell whose mass is equal to the mass deficit in the void), the dense shell typically fragments into large massive clumps (White and Ostriker 1990). In this paper we investigate the self-similar evolution of negative perturbations for all positive values of s . Our main focus is spherically symmetric perturbations, but, in order to see how the evolution depends on geometry, we also present the main features of planar and cylindrical perturbations.

The paper is outlined as follows. In §2 we write the equations of motion and transform them into the appropriate self-similar form. In §3 we derive the asymptotic behavior of the equations for various values of s , and the adiabatic indexes, γ . In §4 the qualitative features of the numerical solution are described. In §5 we check the possibility of structure formation in collisionless and baryonic shells. In §6 we consider evolution of shells, whose expansion is dominated by an internal pressure source. In §7 we present the summary of our results.

2 THE EQUATIONS

We write the Newtonian equations of motion governing the adiabatic evolution of symmetric perturbations in a collisional fluid (gas) of adiabatic index γ . We assume that the expansion scale factor of the universe is $a(t) \propto t^{2/3}$, where t is the age of the Universe, the Hubble function is $H(t) = 2/(3t)$, the total background density is $\rho_c = 3H^2/(8\pi G) = 1/(6\pi Gt^2)$, and the ratio of the mean collisional baryonic density to the critical density ρ_c is denoted by Ω_b . Although self-similar evolution exists for any $\Omega_b \leq 1$, in this paper we restrict the analysis to either $\Omega_b = 1$, or $\Omega_b \ll 1$.

Denote by r and $v \equiv dr/dt$ the physical position and velocity of a gas shell, where $r = 0$ is the symmetry center of the perturbation. Further, let $\rho(r, t)$ and $p(r, t)$ be the gas density and pressure at r . We write the mass within a distance r from the symmetry center as $m(r, t) = \int_0^r x^{n-1} \rho(x, t) dx$, where $n = 1, 2$, and 3 refer, respectively, to planar, cylindrical, and spherical perturbations. The mass within a fixed shell varies with time like $m \sim t^{-2(3-n)/3}$, because of the Hubble expansion along $3 - n$ of the axes. At this stage we neglect such physical effects as viscosity, thermal conduction, cooling etc., so the equations of motion of collisional fluid are, the continuity equation,

$$\frac{d}{dt} \left[\rho t^{\frac{2(3-n)}{3}} \right] = -t^{\frac{2(3-n)}{3}} \rho r^{1-n} \partial_r (r^{n-1} v), \quad (1)$$

the Euler equation,

$$\frac{dv}{dt} - \frac{2}{9} \frac{3-n}{n} \frac{r}{t^2} = -\frac{\partial_r p}{\rho} - \frac{4\pi G m_x}{r^{n-1}}, \quad (2)$$

the adiabatic condition,

$$\frac{d}{dt} (p \rho^{-\gamma}) = 0, \quad (3)$$

and the relation,

$$\partial_r m = r^{n-1} \rho. \quad (4)$$

In equation (2), m_x stands for total (collisional and collisionless) mass.

There are several similar techniques, which we do not describe here in detail, for calculating the collisionless mass profile (Bertschinger 1985; Fillmore & Goldreich 1984). The main idea is that, since the motion is self-similar, knowing the orbit of a single particle one can calculate the mass profile and vice versa. Given the initial guess for mass profile, after iterative calculation of mass profile and orbit one arrives to the self-similar solution.

The initial conditions leading to self-similar expansion are specified at an early time close to zero, t_i , as

$$\frac{\delta M}{M} = - \left(\frac{r}{r_0} \right)^{-s}, \quad r \gg r_0 \quad (5)$$

$$v(r, t_i) = \frac{2}{3t_i} r, \quad (6)$$

$$p(r, t_i) = 0, \quad (7)$$

where $s > 0$ and $\delta M/M$ is the mean density contrast interior to r . The Einstein-De Sitter Universe and the initial conditions are completely scale-free. The only characteristic length in the evolution of the perturbation is the scale of non-linearity $r_*(t)$. For self-similar collapse of positive perturbations the turn-around radius is usually used as the scale of non-linearity. For a negative perturbation, r_* can be defined at any time as the radius interior to which the mean density contrast has a certain fixed value. This means that

$$r_* \propto t^\alpha, \quad \alpha = \frac{2s}{3(s+1)}. \quad (8)$$

This is also the way the turnaround radius in positive perturbation depends on time. The choice of proportionally factor in (8) is arbitrary. Here it is chosen such that a particle with initial radius r_i reach r_* at $(6\delta M/M)^{-3/2} t_i$, where the factor of 6 is arbitrary. For this choice of r_* the mean density contrast interior to r_* is approximately -0.09 in all symmetries.

A consequence of self-similarity is that the partial differential equations of motion can be transformed into ordinary differential equations. This is done by working with $\lambda \equiv r/r_*$ and the dimensionless fluid variables,

$$v(r, t) = \frac{r_*}{t} V(\lambda) \quad (9)$$

$$\rho(r, t) = \Omega_b \rho_c D(\lambda) \quad (10)$$

$$p(r, t) = \Omega_b \rho_c \left(\frac{r_*}{t} \right)^2 P(\lambda) \quad (11)$$

$$m(r, t) = \frac{1}{3} \Omega_b \rho_c r_*^n M(\lambda). \quad (12)$$

Expressed in terms of these variables, the equations (1-4) become, respectively,

$$(V - \alpha \lambda) D' + \left(\frac{n-1}{\lambda} V + V' - \frac{2n}{3} \right) D = 0, \quad (13)$$

$$(\alpha - 1)V + (V - \alpha\lambda)V' - \frac{2}{9} \frac{3-n}{n} \lambda = -\frac{P'}{D} - \frac{2}{9} \frac{M}{\lambda^{n-1}}, \quad (14)$$

$$\left(\gamma \frac{D'}{D} - \frac{P'}{P} \right) (V - \alpha\lambda) = 2(\alpha - 2 + \gamma), \quad (15)$$

$$M' = 3\lambda^{n-1}D, \quad (16)$$

where the prime symbol denotes derivatives with respect to λ .

Self-similarity implies that the shock appears (if it does) at fixed $\lambda = \lambda_s = r_s/r_*$, so the physical radius of the shock $r_s \propto t^\alpha$ and its non-dimensional speed is $(r_*/t)^{-1}(dr_s/dt) = \alpha\lambda_s$. At the surface of the shock the fluid variables satisfy the jump conditions obtained from mass, momentum, and energy conservation (cf. Spitzer 1978, §10.2):

$$\frac{v'_+}{v'_-} = \frac{\rho_-}{\rho_+} = \frac{\gamma - 1}{\gamma + 1}, \quad (17)$$

$$p_+ + \rho_+ v_+^2 = p_- + \rho_- v_-^2, \quad (18)$$

$$v_- = v'_- + \frac{dr_s}{dt}, \quad (19)$$

$$v_+ = v'_+ + \frac{dr_s}{dt}, \quad (20)$$

where the superscripts of the minus and plus signs refer to pre- and post-shock quantities and v' is the velocity relatively to the shock position.

In terms of the non-dimensional fluid variables we obtain

$$V^+ = \alpha\lambda_s + \frac{\gamma - 1}{\gamma + 1}(V^- - \alpha\lambda_s), \quad (21)$$

$$D^+ = \frac{\gamma + 1}{\gamma - 1}D^-, \quad (22)$$

$$P^+ = \frac{2}{\gamma + 1}D^-(V^- - \alpha\lambda_s)^2. \quad (23)$$

Outside the shock, at $\lambda > \lambda_s$, the pressure vanishes and the pre-shock fluid variables can be found by solving the equations (13-16) with zero pressure. Analytic solutions for zero pressure exist for planar and spherical geometries, but not for cylindrical (Zel'dovich 1970, Peebles 1980, Bertschinger 1985).

2.1 The existence of shocks and the value of s

Lower and upper limits on s exist for a shocked expansion of an isolated negative cosmological perturbation. A necessary condition for the formation of a shock is that the perturbation is steep enough so that inner shells expand faster than outer shells. An inspection of the equations of motion shows that this happens only if $(\alpha - 1)\alpha < \frac{2}{9} \frac{3-n}{n}$, that is $s > 2$ for spherical, $s > 1.54$ for cylindrical, and $s > 1$ for planar symmetry. This lower limit disappears if an external energy source is placed at the center of the perturbation.

An upper limit on s also exists. To see this, consider the case of a spherical perturbation. If the perturbation is negative, the total energy of a particle is positive and so

the energy inside the shock must increase as it sweeps more particles. On the other hand, self-similarity implies that the total energy within λ_s varies with time as $t^{5\alpha-4}$ which is a decreasing function of time for $\alpha < 4/5$, i.e., $s < 5$. To satisfy both conditions the energy within λ_s must be negative. The only way to construct such system is by placing a bound object (i.e., negative energy) at the center. However, since there is no way to make this object grow with time, the evolution of the perturbation never becomes self-similar. The limiting case of $s \rightarrow 5$, which corresponds to a shock in a homogeneous medium (compensated void), was investigated by Bertschinger (1983). The corresponding upper limits for cylindrical and planar perturbations are $s \approx 3.5$ and $s = 2$, respectively.

2.2 Boundary conditions

Solving the self-similar equations (13-16) requires boundary conditions on the fluid variables. We will see in the next section that shocked expansion is associated with a dense shell whose outer boundary is the shock. Outside the shock the pressure is zero and the equations can be solved by standard numerical techniques. The jump conditions (21-23) provide post-shock fluid variables. Given the post-shock fluid variables, the equations (13-16) can be integrated inward to obtain the fluid variables inside the shock.

So far it seems that one can introduce the shock at any arbitrary radius. However, inward integration of the equations from an assumed shock position always end at a singular point, λ_0 , where at least one of the fluid variables becomes infinite. Since there is no natural way of eliminating this singularity, this must be the inner boundary of the baryonic shell, $M_{gas}(\lambda_0) = 0$. If the total energy of the system is to be conserved, the pressure at the inner boundary of the system must be zero, $P(\lambda_0) = 0$, otherwise, energy will continuously be injected into the system. It turns out that there is at most one value of λ_s , for which the solution satisfies $P(\lambda_0) = 0$. Smaller values of λ_s give positive mass and pressure at λ_0 , while larger values give zero mass and positive pressure.

3 ASYMPTOTIC BEHAVIOR NEAR THE INNER BOUNDARY OF THE SHELL

3.1 Baryonic matter

To obtain an asymptotic behavior for the collisional matter we expand the fluid variables near λ_0 , as

$$M(\lambda) = M_0(\lambda - \lambda_0)^\mu$$

$$D(\lambda) = D_0(\lambda - \lambda_0)^\delta$$

$$P(\lambda) = P_0(\lambda - \lambda_0)^\eta$$

$$V(\lambda) = \alpha\lambda_0 + V_0(\lambda - \lambda_0)^\nu$$

By substituting these expressions in the equations of motion we find that $\nu = 1$ in all cases(cf. Ostriker & McKee 1988), while δ , μ and η depend on s and γ . The asymptotic

exponents of the fluid variables in the mixed and purely collisional matter are the same. This differs from the collapse case where the collisional component can change the asymptotic exponents of the collisional fluid variables near the center (Chuzhoy & Nusser 2000). Table 1 lists the asymptotic exponents for the following three cases:

I. Expansion without a shock, $\lambda_0 = 0$: As we have mentioned in the previous section, there are no solutions with a shock for $(\alpha - 1)\alpha \geq \frac{2}{9}\frac{3-n}{n}$ with $P(\lambda_0) = 0$. The expansion then develops without a shock and the pressure vanishes everywhere. Substituting the asymptotic form for the fluid variable with $\lambda_0 = 0$, in the equation of motion yields the asymptotic exponents in this case as listed in Table 1. Near $\lambda = 0$, the mass vanishes and the velocity grows linearly as $V_0\lambda$, where V_0 is independent of s .

II. Shocked expansion with $P(\lambda_0) = 0$: This occurs if $(\alpha - 1)\alpha < \frac{2}{9}\frac{3-n}{n}$, i.e., if $s > 2$ for spherical, $s > 1.54$ for cylindrical and $s > 1$. For these values of s the exponent δ as given in table 1 is always negative and so the density diverges at λ_0 .

III. Shocked expansion with $P(\lambda_0) > 0$: This occurs when energy can be injected from the center of the perturbation (e.g., SN energy injection) allowing $P(\lambda_0) = \text{const} > 0$ at the inner shell boundary. The asymptotic behavior for this case is also listed in the table.

3.2 Collisionless matter

After going through first shell-crossing, a collisionless particle starts its converging oscillatory motion around some λ_x inside the dense shell (Fillmore & Goldreich 1984). At each turnaround point there is a caustic peak, where the density diverges. To obtain the asymptotic solution at the caustic we again expand the variables around the peak location

$$\begin{aligned} M(\lambda) &= M_0(\lambda - \lambda_0)^\mu \\ D(\lambda) &= D_0(\lambda - \lambda_0)^\delta \\ P(\lambda) &= 0 \\ V(\lambda) &= \alpha\lambda_0 + V_0(\lambda - \lambda_0)^\nu. \end{aligned}$$

Substituting into the continuity, Euler and mass equations, we obtain $\mu = 1/2$, $\delta = -1/2$, $\nu = 1/2$ and $V_0^2 = 2(1 - \alpha)\alpha\lambda_0$. Negative and positive V_0 correspond to the incoming and out-coming streams at the caustic. Note that, unlike the collisional case, the asymptotic exponents depend neither on symmetry nor value of s .

4 NUMERICAL SOLUTIONS

In order to obtain the detailed structure of the baryonic shell we numerically integrate the self-similar equations of motion (13-16). The location of the shock, λ_s , is sought by demanding vanishing pressure at the inner boundary of the baryonic shell. Integrating the equations inwards from arbitrary λ_s always leads to a singular point, where the derivatives of the fluid variables diverge. If the assumed λ_s is larger than the desired value, then at this point pressure is positive and

Table 1. Asymptotic constants, V_0, δ, η collisional fluid variables in a flat universe with no collisionless matter.

	$\lambda_0 = 0$	$\lambda_0 > 0$	$\lambda_0 > 0$
	NO SHOCK	$P(\lambda_0) = 0$	$P(\lambda_0) > 0$
δ	$\frac{ns(\sqrt{n}-\sqrt{n+24})}{s\sqrt{n+24}-(s+4)\sqrt{n}}$	$\frac{n-2-s(3\gamma-4)}{2+n(\gamma-1)+s(3\gamma-4)}$	$-\frac{s(3\gamma-4)+2}{2+n\gamma+s(3\gamma-4)}$
μ	$\delta + 3$	$\delta + 1$	$\delta + 1$
η	$P = 0$	$\delta + 1$	
V_0	$\frac{3\sqrt{n}+\sqrt{n+24}}{6\sqrt{n}}$	$\frac{2(n-2+\gamma(1-n))+2s(\gamma-2)}{3\gamma s}$	

mass is zero, while if it is smaller then the mass is also positive. Thus it is possible to find λ_s iteratively starting from the initial guess and varying it in accordance with the results of the integration. We will show numerical results for only two cases $\Omega_b = 1$ and $\Omega_b \ll 1$. To find the solution for $\Omega_b \ll 1$ we need the mass profile for the purely collisionless collapse. This is found using the method of Fillmore&Goldreich(1984) and Bertschinger(1985).

Figures 1-2 show the shock location and thickness as a function of s . Figure 3 shows the fluid variables as a function of λ for several values of s . All the plots were made for a spherical expansion with $\gamma = 5/3$. All the numerical solutions we found conform near the inner boundary of the shell to the results of asymptotic analysis. The location of the shock (fig. 1) depends strongly on s but is nearly independent of both of γ and Ω_b . The reason for this weak dependence on γ is that the thermal energy is small to the kinetic and gravitational energies. The thermal energy and hence the width of the shell increase with s (fig. 2), from zero to a few per cent of the void radius. The baryonic shell lies in the collisionless shell. Because the collisionless particles are not slowed down as they enter the shell, the collisionless shell is typically several times wider than the baryonic shell.

5 FRAGMENTATION

5.1 Baryonic matter

We address the question whether the shells can fragment into bound objects, such as galaxies.

For the expansion of an object to halt, its gravitational energy must be larger than the sum of the thermal and the kinetic energy by some finite factor, i.e.

$$E_g + C_f(E_k + E_t) < 0 \quad (24)$$

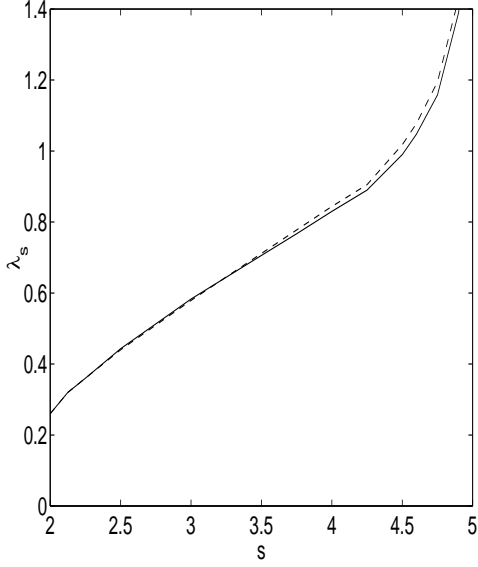


Figure 1. The shock location λ_s as a function of s . The dashed and the solid line correspond, respectively to $\Omega_b = 1$ and $\Omega_b \ll 1$.

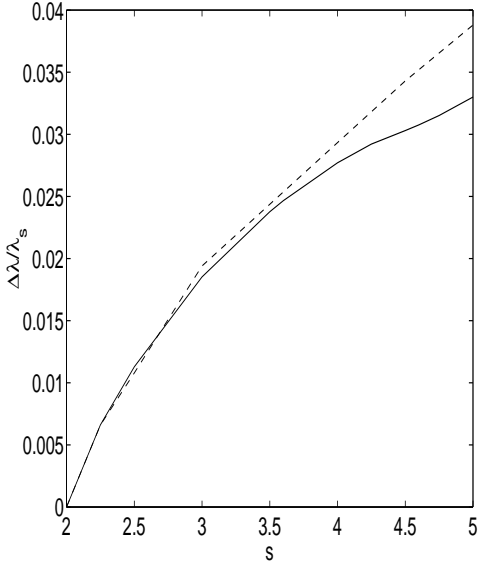


Figure 2. Shell width $\Delta\lambda/\lambda_s$ as a function of s . The solid and the dashed line correspond, respectively to $\Omega_b = 1$ and $\Omega_b \ll 1$.

To check whether an object satisfying the above equation can be found, we calculate the energy of a disk placed on the interior boundary of the shell (where the density is highest and the temperature is lowest).

Let the disk be of radius $l = r_* L$ and height $h = r_* H$.

The kinetic energy due to the shear velocity is found to be

$$E_k = C_n m_d \left(\frac{l}{2t}\right)^2 = \left(\frac{r_*^5}{6t^4}\right) \Omega_b M L^4 \frac{C_n}{12\lambda_0^2}, \quad (25)$$

where $C_n = 4/9$, $(2/9 + \alpha^2/2)$, and α^2 for $n = 1, 2$, and

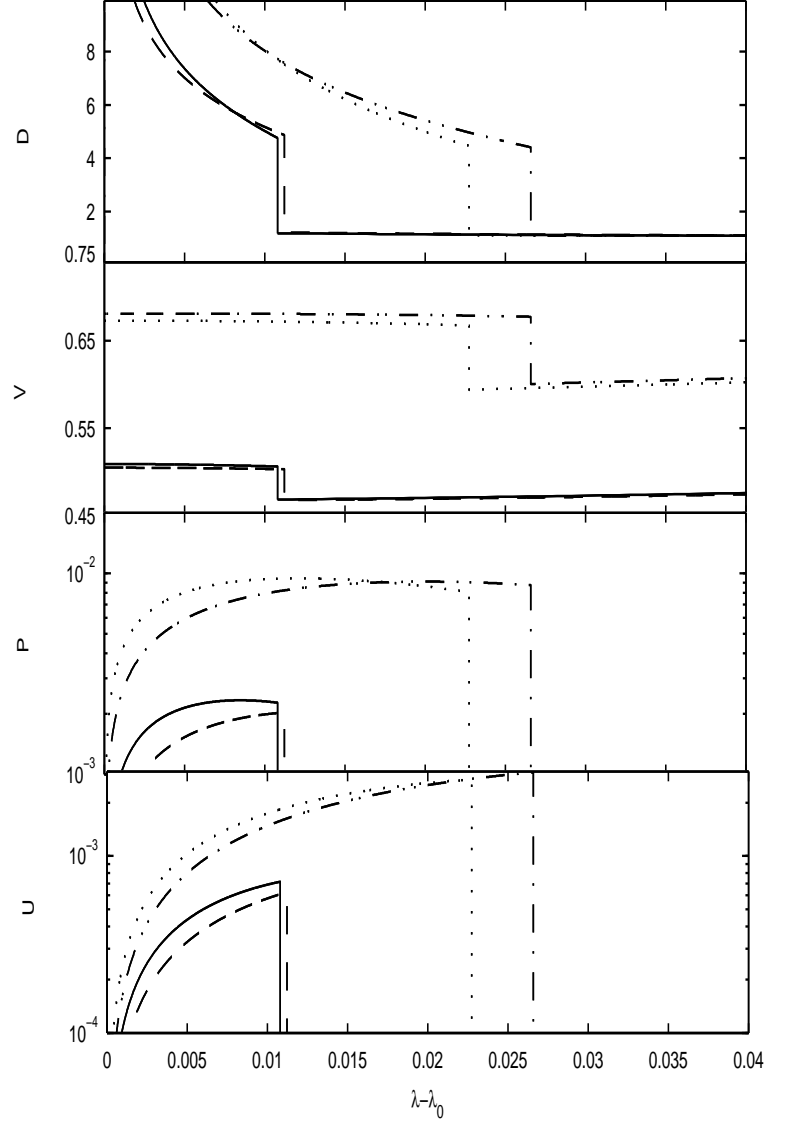


Figure 3. The fluid variables (density, velocity, pressure and thermal energy) for the case of spherical symmetry and $\gamma = 5/3$. The solid and dotted lines correspond to $\Omega_b = 1$ with $s = 3$ and $s = 4$ respectively, dashed and dash-dotted lines correspond to $\Omega_b \ll 1$ with $s = 3$ and $s = 4$.

3, respectively and $m_d \approx \frac{\pi l^2}{3r_*^2} M \Omega_b \rho_c r_*^3$ is the mass of the disk.

The gravitational energy is obtained using the thin shell approximation * -

$$E_g = -\frac{8m_d^2}{3\pi l} = -\left(\frac{r_*^5}{6t^4}\right) \frac{4}{81\pi} \Omega_b^2 L^3 \frac{M^2(\lambda_0 + H)}{\lambda_0^4} \quad (26)$$

The thermal energy -

* For all the disks satisfying (24), that we found, $H \ll L$. Thus, since the correction for finite thickness of the disk lowers the gravitational energy, the assumption of a thin disk is justified.

$$E_t = \int \frac{\pi}{\gamma-1} l^2 p dr = \left(\frac{r_*^5}{6t^4}\right) \frac{\Omega_b}{\gamma-1} L^2 \int_{\lambda_0}^{\lambda_0+H} P d\lambda \quad (27)$$

The kinetic energy due to the radial velocity -

$$E_{k2} = \int \pi l^2 \rho (v - \langle v \rangle)^2 / 2 dr = \quad (28)$$

$$= \left(\frac{r_*^5}{6t^4}\right) \Omega_b L^2 \int_{\lambda_0}^{\lambda_0+H} D (V - \langle V \rangle)^2 / 2 d\lambda, \quad (29)$$

where $\langle V \rangle$ is an average radial velocity of the disk. From the asymptotic analysis follows that $E_{k2}/E_t \propto H$, so for $H \ll 1$ we can neglect E_{k2} .

For large values of L the kinetic energy term, $E_k \propto L^4$, would be dominant, while for small L the thermal energy, $E_t \propto L^2$, is the only significant term. Thus the disk can be unstable only for intermediate values of L , where the gravitational term, $E_g \propto L^3$, is dominant. From eq. (24) we can factor an equation of second degree in L , whose roots determine the limits of instability for a given thickness of the disk, H . The condition for the existence of the roots is

$$16\Omega_b(\gamma-1) \frac{M^3}{\lambda_0^6} > 3^7 \pi^2 C_n C_f^2 \int_{\lambda_0}^{\lambda_0+H} P d\lambda \quad (30)$$

5.1.1 Fragmentation without cooling

The asymptotic solution implies that the term on the l.h.s. of eq. 30 grows as $H^{3(\delta+1)}$ and the right as $H^{\delta+2}$ and thus in the limit $H \rightarrow 0$ the inequality is satisfied if $\delta < -\frac{1}{2}$.

For $\gamma = 5/3$, δ is less than $-\frac{1}{2}$ for all planar shocks and for cylindrical shocks with $s > 10/3$, which are consequently gravitationally unstable even for $\Omega_b \ll 1$. For spherical shocks δ is less than $-\frac{1}{2}$ only in case the shell pushed by an internal pressure source with expansion rate $\alpha < 8/9$. For spherical shocks with $P(\lambda_0) = 0$ the numerical integration shows that for $\Omega_b = 1$ and $C_f = 1$ eq. (30) is satisfied only for $s > \sim 3.5$ and not at all if $\Omega_b < 0.8$.

5.1.2 Fragmentation with cooling

From the numerical calculation we find that for a disk on a spherical shell with zero internal pressure to satisfy eq.(30) its thermal energy must fall at least by factor Ω_b^{-1} . To check when this is indeed possible we must introduce a physical scale into the problem.

The physical temperature of the shock for ionized gas is

$$T \approx \frac{P_s}{D_s \lambda_s^2} \frac{0.6 m_p}{k_B} \left(\frac{r_s}{t}\right)^2 \quad (31)$$

For spherical symmetry the value of $P_s/D_s \lambda_s^2$ can be approximated by $(s-2)/10^3$ for shell driven by negative density perturbation (fig. 4) or by $3(\alpha-2/3)^2/16$ for shell driven by internal pressure. Thus

$$T \approx 2(s-2)10^5 r_{10}^2 (1+z)^{(s-2)/s} K \quad (32)$$

or

$$T \approx 4(\alpha-2/3)^2 10^7 r_{10}^2 (1+z)^{3(1-\alpha)} K, \quad (33)$$

where $r_{s0} = 10r_{10}$ Mpc is the present radius of the shock.

At temperatures higher than $\sim 10^4 K$ and densities not much higher than the background values the inverse Compton scattering is the dominant cooling process. At redshifts $\gtrsim 8$ the cooling time $t_{cool} = 1.6 \cdot 10^{12} (1+z)^{-4} \text{Yr}$ (Bertschinger 1983) is less than the age of the universe. This means that the gas shock cools quickly after the shock and the average temperature of the shell remains at constant value of order of $10^4 K$. Thus the approximate condition for fragmentation is for the shock temperature to be higher than $\sim 10^4 \Omega_b^{-1} K$.

When the collapse depends on cooling the mass of the formed objects is of order of Jeans mass at $T \sim 10^4 K$, i.e., $M \sim 10^{11} \Omega_b^{-1/2} (1+z)^{-3/2} M_\odot$. Since the mass accretion rate on the shell is proportional to $(1+z)^{9(1-\alpha)/2}$, the number of objects of the mass M formed by the shell is proportional to $N(M) \propto M^{2\alpha-3}$.

It should be noted that different equations of motion (Appendix A) are needed to describe the shell that loses its thermal energy during fraction of its dynamic time (snow-pow). The main effect of the cooling is to move the shock inwards thus decreasing the swept mass and the shock temperature. However, since in this problem the thermal energy constitutes only a small fraction of the total, these differences are generally insignificant.

5.2 Collisionless matter

We now address the stability condition of the collisionless shell. The kinetic and gravitational energy terms are the same as in the baryonic case. There are two stream flows near λ_0 (cf, section 3.2), so the ‘‘thermal’’ energy resulting from the velocity dispersion in the flow is $E_t = \frac{r_*^5}{6\pi t^4} \frac{\pi}{2} L^2 \int_{\lambda_0}^{\lambda_0+H} D (V - \alpha\lambda)^2 d\lambda$. The analog of eq. 30 for this case is

$$32 \frac{M^3}{\lambda_0^6} > 3^7 \pi^2 C_f^2 C_n \int_{\lambda_0}^{\lambda_0+H} D (V - \alpha\lambda)^2 d\lambda \quad (34)$$

Near the inner boundary both the left and the right term grow as $H^{3/2}$ and thus the fact whether the last inequality is satisfied depends on the choice of C_f . However, using just the lower constraint $C_f > 1$, we found that for small H it is never satisfied in the case of spherical symmetry. For large H the energy analyses must give the same results for pure collisional ($\Omega_b = 1$ and $\Omega_c = 0$) and pure collisionless ($\Omega_b = 0$ and $\Omega_c = 1$) models. Thus we expect the bound structures to form for all s in planar shells, for $s > \sim 3$ in cylindrical shells, and possibly for $s > \sim 3.5$ in spherical shells.

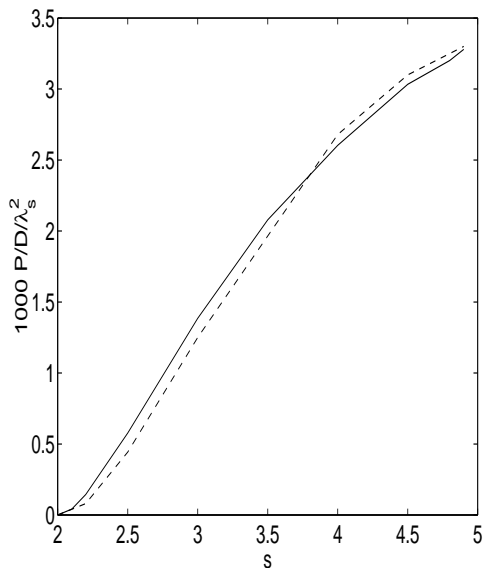


Figure 4. Non-dimensional shock temperature as a function of s (eq. 31). The solid and the dashed line correspond, respectively, to $\Omega_b = 1$ and $\Omega_b \ll 1$.

6 EXPLOSIVE AMPLIFICATION

The explosive amplification model suggesting that galaxies can originate from series of explosions was proposed by Ostriker & Cowie (1981) and later developed by other authors. Vishniac, Ostriker & Bertschinger (1985) showed that an energy injection from supernova explosions in the range $10^{57} - 10^{61}$ could produce a void reaching ~ 10 Mpc. The cooling of the shell surrounding the void would then lead to the formation of galaxies. However, since the cooling proceeds chiefly through inverse Compton scattering, it was argued that a large number of such explosions would be incompatible with the observational limits on the Compton y -distortion parameter (Levin, Freese & Spergel 1992). Later Miranda & Opher (1997) showed that if the energy was injected in several rather than in a single cycle, then the distortion would be several times smaller. In their calculation the current observational limit $y \lesssim 1.5 \cdot 10^{-5}$ (Fixen et al. 1996) is compatible with voids of present radii $R \sim 10 - 30$ Mpc, the filling factor $f_F \sim 0.07 - 0.30$, and $\Omega_b = 0.1$. In this section we explain how the distortion produced by shocks of similar size might be still lower by one or two orders of magnitude.

In the previous section we have shown that before $z \sim 8 - 10$ large baryonic shells become gravitationally unstable. The collapse of one object creates a pressure gradient causing the surrounding gas to expand and thus creates a feedback against further collapse. Therefore we expect that fragmentation proceeds continuously rather than in cycles. Depending on the star formation efficiency in the collapsed objects and the fraction of stars turned to supernovae (SN), the dynamics of the shell might become dominated by the energy input from the SN explosions. By using the approximation $L_{inj} \propto \dot{m}_s t^q$, where L_{inj} is the energy injection rate and \dot{m}_s is the mass accretion rate on the shell, we get the expansion rate of the shell $r_s \propto t^\alpha$, where $\alpha = 1 + q/2$. Note

that if mass to energy conversion efficiency doesn't change drastically over time, then $q \approx 0$ and $\alpha \approx 1$.

If the shell expansion is dominated by internal pressure then the collapsing objects, whose surface area is decreasing, would be eventually overtaken by the shell and, unless $\Omega_b \sim 1$, remain inside. Since the interior of the shell is empty of gas, only a small fraction of the SN energy is turned into a thermal energy, making the CBR distortion in this scenario much smaller than in previous models (see Appendix B). Similarly, because less energy is lost through cooling, larger voids can be produced for the same mass to energy conversion efficiency. In this case the radius of the baryonic shell is $R \approx 10h^{-1}(\frac{\epsilon}{10^{-8}})^{1/2}(1+z)^{-3/2}$ Mpc, where $\epsilon = E_{inj}/m_{shell}c^2$.

7 SUMMARY

For the gaussian initial density field with scale free power spectrum the rms density perturbation is $\langle (\frac{\delta M}{M})^2 \rangle \propto r^{-(n+3)}$, where $-3 < n < 4$. It is therefore reasonable to identify $s = (n+3)/2$, from which follows $0 < s < 3.5$. Thus in case $n > 1$ we might expect that the universe contains a large number of spherical shells. We have shown in the paper that the evolution of spherical perturbations with $s > 2$ results in formation of overdense regions, which, unless $(s-2) \ll 1$ may contain a large fraction of matter.

A distinctive property of structure formation in the shell is the segregation between the baryons and the collisionless matter. The energy analysis shows that for $s < 3.5$ (i.e. $n < 4$), which follows from the gaussian density field, the collisionless matter cannot form bound objects, while at high redshifts cooling allows formation of the baryonic objects on the appropriate scales. Similarly, the explosive model (§6) predicts that the baryonic shell is driven by pressure ahead of the collisionless and fragments in an independent way. This is entirely different from the evolution of positive perturbations, where gas must fall into the potential well formed by collisionless matter.

The energy analysis (§5.1.2) shows that the mass of the bound objects formed from the baryonic shell is of order of Jeans mass at $T \sim 10^4 K$ - $M \sim 10^{11} \Omega_b^{-1/2} (1+z)^{-3/2} M_\odot$. This is again different from the evolution of positive perturbation, which predicts the Jeans mass to be also dependent on the spectrum of perturbations.

An observational limit on the scale and number of the shells can be obtained from the amplitude of Compton y -distortion. Both for the shell driven by the negative density perturbation and for the shell driven by internal pressure the predicted amplitude is of order $10^{-5} \frac{\Omega_b}{0.1} (\frac{r_{10}}{3})^2 f_F$, where f_F is the present filling factor (see Appendix B for the details of the calculation).

The current upper limit $y = 1.5 \cdot 10^{-5}$ is thus consistent with shells, whose present radius is below ~ 30 Mpc and the filling factor is of order of unity.

8 ACKNOWLEDGMENT

This research was supported by the Technion V.P.R Fund-Henri Gutwirth Promotion of Research Fund, the German-Israeli Foundation for Scientific Research and Development, and the Israeli Science Foundation.

REFERENCES

- Bertschinger E., 1983, ApJ, 268, 17
Bertschinger E., 1985, ApJS, 58, 1
Chuzhoy L., Nusser A., 2000, MNRAS, 319, 797
Fillmore J.A., Goldreich P., 1984, ApJ, 281, 9
Fixen K.J. et al. 1996, ApJ, 473, 576
Hwang J., Vishniac E.T., Shapiro P.R., 1989, 346, 12
Levin J.J., Freese K, Spergel D.N. 1992, ApJ, 389, 464
Miranda D.M., Reuven O. 1997, ApJ, 482, 573
Ostriker J.P., Cowie L.L. 1981, ApJ, 243, L127
Ostriker J.P., McKee C.F. 1988, Rev.Mod.Phys.,60,1
Ryden B. S., 1994, ApJ, 423, 534
Spitzer L. 1978, Physical Processes in the Interstellar Medium
(New York: Wiley-Interscience)
White S.D.M., Ostriker J.P., 1990, ApJ, 349, 22
Vishniac E.T., ApJ, 1983, 274, 152
Vishniac E.T., Ostriker J.P., Bertschinger E. 1985, ApJ, 291, 399
Zel'dovich Ya.B., A&A, 1970, 5, 84

APPENDIX A: EXPANSION OF A THIN MOMENTUM CONSERVING SHELL (SNOW PLOW)

If the cooling time is much shorter than the dynamical time of the system the shocked gas would be compressed into a thin shell, whose expansion can still be described in self-similar form ($r_s = r_{s0}t^\alpha$). Given the initial density profile and energy injection rate, the constants α and r_{s0} can be determined using momentum conservation, i.e.,

$$\frac{d(mt^{2-2n/3\alpha r/t})}{dt} = \frac{2(3-n)}{9n} \frac{mt^{2-2n/3}r}{t^2} - \frac{2\pi(m+2m_c)mt^{2-2n/3}}{r^{n-1}} - \rho r^{n-1}(v - \alpha r/t)vt^{2-2n/3} + f_p, \quad (\text{A1})$$

where f_p is the force of the internal pressure, ρ and v are the density and the velocity of the gas just outside the shock, and m and m_c are, respectively, the masses of baryonic and collisionless components. In the dimensionless form (A1) is expressed as,

$$6\alpha(\alpha - 1 + n(\alpha - 2/3)) = \frac{2(3-n)}{n} - C \frac{M}{\lambda^n} + \frac{27DV(\alpha\lambda - V)\lambda^{n-2}}{M} + \frac{F_p}{M\lambda}, \quad (\text{A2})$$

where $C = 2$ for $\Omega_b \ll 1$ (if the baryonic shell is ahead of the collisionless) and $C = 1$ for $\Omega_b = 1$.

If the expansion is caused by instantaneous energy injection then α is found by substituting $M = 3\lambda/n$, $D = 1$, $V = 2\lambda/3$ and $F_p = 0$ in (A2). The result is

$$\alpha = \frac{3 + 4n + \sqrt{(24 + 25n - 12C(n+1))/n}}{6(n+1)}. \quad (\text{A3})$$

For $\Omega_b = 1$ α is equal respectively to 0.797 for spherical symmetry, 0.853 for cylindrical and 1 for planar symmetry. For $\Omega_b \ll 1$ and the baryonic shell is ahead of the collisionless $\alpha \approx 2/3 + \Omega_b/2n$.

If on the other hand the expansion is caused by negative density perturbation or a continuous energy injection then while α is the same as in the adiabatic case where cooling is negligible. This is because the thermal energy is only a small fraction of the total energy anyways. Cooling however causes a slight decrease in r_{s0} .

APPENDIX B: SHOCK IMPRINT ON THE COSMIC BACKGROUND RADIATION

The spectral distortion of the cosmic background radiation (CBR) is given by

$$y = \frac{\Delta T}{2T} = \int \frac{k_B T_e}{m_e c^2} \sigma_T n_e dl, \quad (\text{B1})$$

where n_e and T_e are the electron density and temperature and σ_T is the Thompson cross section for photon electron scattering.

Averaging over a spherical volume gives $\langle dy/dl \rangle = \sigma_T E_{th}/(4\pi m_e c^2 r_s^3)$, where E_{th} is the thermal energy of the entire shell.

Prior to $z \lesssim 8$ the shell cools quickly so its thermal energy may be approximated by

$$E_{th} \approx \int_0^\infty \frac{6\pi\dot{m}_s}{\mu} k_B T_s e^{-t/t_{cool}} dt = \frac{6\pi\dot{m}_s}{\mu} k_B T_s t_{cool} = \left(\frac{3\alpha - 2}{3} \frac{r_s^5 t_{cool}}{G t^5}\right) \left(\frac{P_s M_s}{D_s \lambda_s^5}\right), \quad (\text{B2})$$

where μ is the mean mass per particle. At later redshifts the thermal energy is $E_{th} = \int_{r_0}^{r_s} 4\pi p r_s^2 dr \approx \left(\frac{2r_s^5}{3Gt^4}\right)(\lambda_s^{-3} \int_{\lambda_0}^{\lambda_s} P d\lambda)$.

The filling factor of the shells grows as $f(t) = f_F t^{3\alpha-2}$, where f_F is the final filling factor, thus the final distortion is,

$$y = \int_{z_i}^{z_f} \frac{dy}{dl} f(t) \frac{dl}{dz} dz. \quad (\text{B3})$$

Both for spherical shells driven by the internal pressure ($4/5 < \alpha < 2$) and shells driven by the negative density perturbation $y \lesssim 10^{-5} f_F r_{10}^2 \Omega_b$, where f_F and $10r_{10}$ Mpc are the present filling factor and radius of the shells.